Robotica (2014) volume 32, pp. 1–17. © Cambridge University Press 2013
doi:10.1017/S0263574713000593

A psychophysical evaluation of haptic controllers: viscosity perception of soft environments

Hyoung Il Son†*, Hoeryong Jung†, Doo Yong Lee‡, Jang Ho Cho§ and Heinrich H. Bülthoff¶‖

†*Institute of Industrial Technology, Samsung Heavy Industries, 217 Munji-ro, Yuseong-gu, Daejeon 305-380, Republic of Korea*
‡*Department of Mechanical Engineering, KAIST, 291 Daehak-ro, Yuseong-gu, Daejeon, 305-701, Republic of Korea. E-mail: leedy@kaist.ac.kr*
§*Department of Automatic Control, Lund University, PO Box 118, SE-221 00 Lund, Sweden. E-mail: jangho@control.lth.se*
¶*Max Planck Institute for Biological Cybernetics, Spemannstraße 38, 72076 Tübingen, Germany. E-mail: hhb@tuebingen.mpg.de*
‖*Department of Brain and Cognitive Engineering, Korea University, Anam-dong, Seongbuk-gu, Seoul 136-713, Republic of Korea*

(Accepted May 23, 2013. First published online: July 19, 2013)

SUMMARY
In this paper, human viscosity perception in haptic teleoperation systems is thoroughly analyzed. An accurate perception of viscoelastic environmental properties such as viscosity is a critical ability in several contexts, such as telesurgery, telerehabilitation, telemedicine, and soft-tissue interaction. We study and compare the ability to perceive viscosity from the standpoint of detection and discrimination using several relevant control methods for the teleoperator. The perception-based method, which was proposed by the authors to enhance the operator's kinesthetic perception, is compared with the conventional transparency-based control method for the teleoperation system. The fidelity-based method, which is a primary method among perception-centered control schemes in teleoperation, is also studied. We also examine the necessity and impact of the remote-site force information for each of the methods. The comparison is based on a series of psychophysical experiments measuring absolute threshold and just noticeable difference for all conditions. The results clearly show that the perception-based method enhances both detection and discrimination abilities compare with other control methods. The results further show that the fidelity-based method confers a better discrimination ability than the transparency-based method, although this is not true with respect to detection ability. In addition, we show that force information improves viscosity detection for all control methods, as predicted from previous theoretical analysis, but improves the discrimination threshold only for the perception-based method.

KEYWORDS: Haptic controller; Telemedicine; Teleoperation; Viscosity perception; Psychophysical evaluation.

1. Introduction

In many biomedical applications such as cell manipulation, (tele) surgery, (tele) rehabilitation, and telemedicine, the sense of touch (i.e., haptics) has a crucial role to play in skilled actions.[1] Haptic feedback, especially in surgical applications, provides sensation to numerous surgical procedures for better performance in task completion time, tissue damage, and straightness of suturing. Note also that the (micro) surgical applications, in particular ophthalmology, otology, micro-vascular surgery, and urology, which require tasks and skills like precise positioning, making incisions, micro-dissections,

* Corresponding author. E-mail: hyoungil.son@kaist.ac.kr, hyoungil.son@gmail.com

and suturing small vessels, require precise detection and discrimination (i.e., perception) abilities in terms of force feedback for effective performance, and are also important for reducing injury and trauma.[2,3] The role of force feedback becomes more important with a limited visual feedback.[4]

The kinesthetic perception of human not only relies on processing information regarding the forces generated by muscles and the associated movements of limbs, but also uses this information to derive cues about other mechanical impedance variables such as stiffness, viscosity, and inertia.[5] It has been reported that there is a loss in perceptual sensitivity when force and displacement, velocity, and acceleration cues are combined to perceive the stiffness, viscosity, and inertia, respectively. The perceptual sensitivity for the impedance variables is considerably lower than the perceptual sensitivity measured for limb movement, position, and force.[5,6] Many researchers have focused on identifying human stiffness perception on environments because basically human perceive the environment kinesthetically via its stiffness (force and displacement-dependent term). Viscosity (force and velocity-dependent term), however, is also just as important as stiffness perception, especially in manipulations of viscoelastic soft tissues and in surgical procedures involving a partially liquid environment.[7,8] Better viscosity perception, in addition to stiffness perception, therefore, becomes critical to increase surgeon's performance in surgical procedures. Note that a velocity-dependent viscosity parameter also strongly influences humans' perception of an environmental roughness.[9]

In the past few decades, a variety of teleoperation systems have been designed to allow human operators to manipulate remote environments and perform tasks from a remote site.[10] In a typical teleoperation scenario, the human operator handles a mechanical device (called haptic device or master) to drive a manipulator (called the slave), which is distantly located. The master can provide haptic feedback to the operator in order to increase the overall control task performance.[11] The conventional control objective of a haptic teleoperation system is known as *transparency*, i.e., the environment impedance should be equal to the transmitted impedance to the operator for perfect transparency.[12] From this perspective, the transparency-optimized control method was introduced and analyzed in refs. [12, 13], which is aimed to achieve the perfect transparency based on their performance and stability robustness.

Recently, some researchers have focused on human operator's perception of environment as a control objective instead of transparency[14–19] for tasks such as telesurgery, which require interaction with soft tissues. One of the main research motivations and backgrounds of these perception-centered teleoperation research is a significant increase of interest in biomedical applications of haptic teleoperation, e.g., a big commercial success of the da Vinci surgical system (Intuitive Surgical Inc., Mountain View, California) and the automatic cell manipulation system.[20] Several perception-centered approaches, therefore, were proposed based on this control philosophy. Çavusoglu *et al.*[14] first proposed a new control objective, *fidelity*, to improve the operator's perception of soft environments using their psychophysical experiment results presented in refs. [21, 22]. They defined fidelity as the sensitivity of the impedance transmitted to the operator to changes in remote environment impedance. And then a fidelity-optimized control method was proposed, where control parameters are optimized to maximize a metric for the fidelity while maintaining system stability.

A similar concept was proposed by Gersem *et al.*[15] to enhance the stiffness perception of the operator in soft-tissue telemanipulation. A scaling approach (between the position and force of the master and the slave) was proposed in refs. [16, 17] to increase stiffness and force discrimination, respectively. Malysz and Sirouspour used nonlinear and filtered force/position scaling and validated the proposed method in experiments using sponge instead of soft tissue.[16] Botturi *et al.* proposed a variable force scaling that depends on the position of the slave manipulator and validated it in psychophysical experiments.[17] While previous research focused solely on the enhancement of discrimination, Son *et al.* proposed a kinesthetic perception-optimized control method that can enhance both detection and discrimination ability based on the work of Çavusoglu *et al.*[18] They experimentally evaluated the proposed method using phantom soft tissues and psychophysical tests by comparing with the Çavusoglu *et al.* method and the Malysz and Sirouspour method, and the transparency-optimized approach in refs. [18, 23], respectively. Recently, the perception-centered approach has been explored in the teleoperation of multiple mobile robots.[24]

Previous perception-centered methods,[15–17] however, only focused on the enhancement of environmental stiffness perception by teleoperator. Otherwise, whenever all mechanical impedances were considered in an environmental model, including stiffness, viscosity, and inertia, the proposed

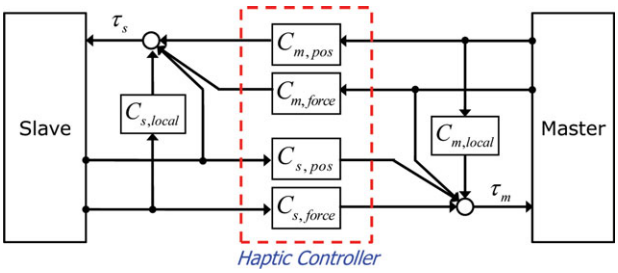

Fig. 1. (Colour online) Schematic of the generalized four-channel control architecture for haptic teleoperation systems.

methods were evaluated only by simulations in ref. [14] or stiffness perception experiments (with a constant viscosity) in refs. [18, 23].

1.1. Objective and organization

In this paper, we will compare and analyze the teleoperator's viscosity perception ability on viscoelastic soft environment, which is affected by *teleoperation control methods*. The viscosity perception ability of the control method proposed by the authors[18] (hereafter the *perception-based method*) will be compared with the conventional approach in refs. [12, 13] (hereafter the *transparency-based method*) and the primary perception-centered approach proposed by Çavusoglu *et al.*[14] (hereafter the *fidelity-based method*). Our comparison is conducted from the standpoints of detection and discrimination. Scaling approaches in refs. [16, 17] were not considered in this work, because we focus on haptic teleoperation systems, one-to-one matching of the dimensions of the human operator and the remote environment.

In teleoperations, additionally, there are several *control architectures*, which are classified according to the information used on the master and the slave side. Basically, two kinds of signals are available on both sides: position and force. If the position signal is used on both the master and slave sides, the architecture is called the position–position (PP) control architecture. In contrast, the force–position (FP) control architecture uses position information only on the master side, while force information is used on the slave side. It is known that FP controllers usually provide a better perception of environments than PP controllers.[14, 18] In some applications such as telesurgery, however, the force information is not usually available for practical reasons such as space limitations and safety as well as low cost.[25] In this paper, therefore, both the PP and FP control architectures are also evaluated for each teleoperation control method.

In this study, we designed two psychophysical experiments to evaluate and compare the perception performance of three types of control methods and two types of control architectures mutually: transparency-based, fidelity-based, and perception-based PP and FP controllers. Detection ability for viscosity was tested by measuring the absolute threshold (AL). The just noticeable difference (JND) was determined to compare the viscosity discrimination ability of each controller.[26] Experimental results will show which haptic teleoperation control method has best and worst performance among PP and FP controllers in the ability to detect and discriminate viscosity. We also analyzed if the force information of the slave manipulator contributes to better performance in viscosity perception as theoretically predicted from previous studies.[14, 18]

The structure of this paper is as follows. First, three control methods and two control architectures are briefly reviewed. Following this, psychophysical experiment methods, including haptic controller design and procedure of the psychophysical experiments, are presented in Section 3. In Section 4, experimental results of the detection and discrimination experiments are presented, with a statistical analysis of those results. Finally, this paper concludes with general discussions and concluding remark.

2. Haptic Controller Design

The generalized four-channel (4C) control architecture of the haptic teleoperation system is presented in Fig. 1. The haptic teleoperation system shown in Fig. 1 consists of the master, the slave, and a

haptic controller. There are four feed-forward controllers in the haptic controller: $C_{m,\text{pos}}$ and $C_{s,\text{pos}}$ are the two position controllers, while $C_{m,\text{force}}$ and $C_{s,\text{force}}$ are the two force controllers controlling the information flow between the master and the slave, respectively. Additionally, there are the local position controllers of the master and slave robots, which are $C_{m,\text{local}}$ and $C_{s,\text{local}}$, respectively. Finally, the control inputs to the master and slave, τ_m and τ_s, respectively, are determined as a function of the haptic controller and the local controller.

Note that, generally, a proportional-derivative (PD) controller is implemented for the position controllers of the haptic controller and the local position controllers because, in practice, acceleration signals are too noisy, as a form of $C_i = K_D s + K_P$, where K_D, $K_P \in \Re^{3\times3}$ are the positive definite and symmetric derivative and proportional gain matrices, while a symmetric scalar gain matrix $K_f \in \Re^{3\times3}$ is defined for $C_{m,\text{force}}$ and $C_{s,\text{force}}$. In this paper, a design of the haptic controller (i.e., a design of $C_{m,\text{pos}}$, $C_{m,\text{force}}$, $C_{s,\text{pos}}$, and $C_{s,\text{force}}$) is referred to as the *control method* while a selection of the information channels in the haptic controller (i.e., a selection among $C_{m,\text{pos}}$, $C_{m,\text{force}}$, $C_{s,\text{pos}}$, and $C_{s,\text{force}}$) is referred to as *control architecture*.

2.1. Control methods

We selected three most relevant control methods: the transparency-based method,[12,13] which is a conventional controller in bilateral teleoperation; the fidelity-based method,[14] which is the primary method among perception-centered approaches in teleoperation; the perception-based method,[18] which was proposed by the authors to enhance the performance of the fidelity-based method. Hereafter, we briefly review these control methods and refer the reader to refs. [12–14, 18] for further details.

2.1.1. Transparency-based method. The transparency is defined as $Z_{to} = Z_e$, where Z_{to} and Z_e represent the transmitted impedance to the operator and the impedance of remote environment, respectively. If a time delay between the master and the slave is negligible, we can achieve perfect transparency using

$$\begin{cases} C_{m,\text{pos}} &= Z_s + C_{s,\text{local}} \\ C_{m,\text{force}} &= 1 \\ C_{s,\text{pos}} &= -Z_m - C_{m,\text{local}} \\ C_{s,\text{force}} &= 1, \end{cases} \tag{1}$$

known as the transparency-optimized control law, where Z_m and Z_s are the master and slave impedances, respectively.

2.1.2. Fidelity-based method. The haptic controller (i.e., $C_{m,\text{pos}}$, $C_{m,\text{force}}$, $C_{s,\text{pos}}$, and $C_{s,\text{force}}$) is optimized by solving a multi-objective constrained optimization problem aimed at maximizing the performance index in (2) of the control objective while guaranteeing stability conditions:

$$P_{\text{fidelity}} := \left\| W_{\text{perception}} \frac{\Delta Z_{to}}{\Delta Z_e} \right\|_2, \tag{2}$$

where $W_{\text{perception}}$ is a low-pass filter. P_{fidelity} measures the sensitivity of the transmitted impedance to changes in the environmental impedance, incorporating human perceptual capabilities.

2.1.3. Perception-based method. Similar to the fidelity-based method, the haptic controller is designed by maximizing the performance index for kinesthetic perception in (3):

$$\begin{aligned} P_{\text{perception}} &:= \left(1 - \tfrac{1}{1+M_{\text{det}}}\right)\left(1 - \tfrac{1}{1+M_{\text{dis}}}\right) \\ \text{where} &\begin{cases} M_{\text{det}} = \left\| W_{\text{perception}} \frac{Z_{to}}{Z_e} \right\|_2 \\ M_{\text{dis}} = \left\| W_{\text{perception}} \frac{\Delta Z_{to}/Z_{to}}{\Delta Z_e/Z_e} \right\|_2. \end{cases} \end{aligned} \tag{3}$$

$P_{\text{perception}}$ measures, unlike with P_{fidelity}, both the ratio of the transmitted impedance to the environmental impedance and the sensitivity of the relative change of the transmitted impedance to relative changes in the environmental impedance via M_{det} and M_{dis}, which are defined based on AL and JND concepts, respectively.

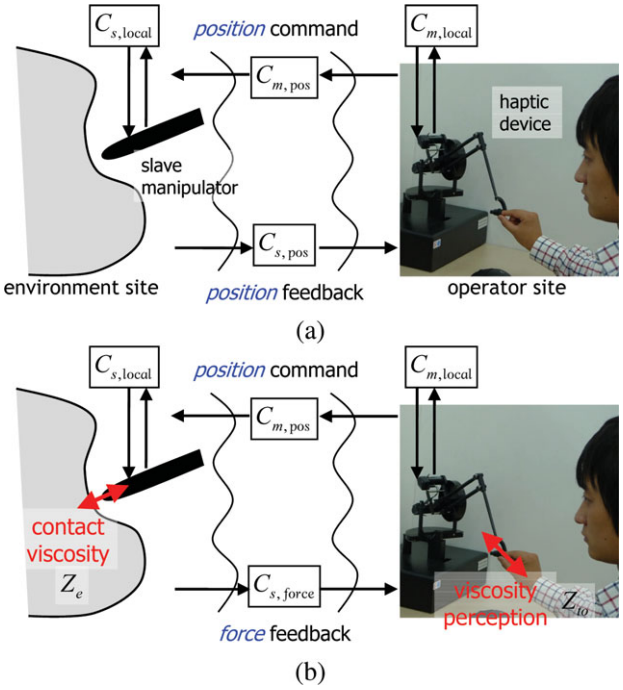

Fig. 2. (Colour online) Schematic of two two-channel control architectures for haptic teleoperation systems. Human operator manipulates a slave located at a remote site by driving a haptic device. The operator perceives the viscosity of an environment through position/force feedback. (a) Position–position control architecture. Position signals are transmitted from/to the haptic device to/from the slave manipulator. (b) Force–position control architecture. Force and position information are transmitted from the slave manipulator to the haptic device and from the haptic device to the slave manipulator, respectively.

Note that the aforementioned optimization problems to maximize P_{fidelity} and $P_{\text{perception}}$ are non-convex in nature and so the convergence to the global optimum is not guaranteed. However, proper selection of models and criteria and a varied range of model parameters with repetitive simulations can make the local optimum very close to the global optimum, and the results so obtained can be satisfactory for our cases.[14,18]

2.2. *Control architectures*

Generally, the force information from the master is unavailable to maintain high performance (e.g., low inertia) of the haptic device and keep a low cost. From this practical perspective, we evaluated two-channel control architectures: the PP and FP control architectures, as illustrated in Figs. 2(a) and (b), respectively.

Both architectures implement two position controllers for the position of the haptic device ($C_{m,\text{local}}$) and the slave manipulator ($C_{s,\text{local}}$). The feed-forward position controller of the master ($C_{m,\text{pos}}$) sends the position command to the environment site in both the PP and FP controllers. In the PP architecture, the position controller of the slave ($C_{s,\text{pos}}$) feeds back the position of the slave, while in the FP architecture the feed-forward force controller ($C_{s,\text{force}}$) sends back the interacting force between the slave and the environment. For more details on control architectures of teleoperation systems refer to ref. [13].

2.3. *Force feedback mechanism*

The interacting force with the environment, $f_s \in \Re^3$ is calculated as

$$f_s = -B_e\dot{x}_s - K_e x_s, \tag{4}$$

where $B_e \in \Re^{3\times3}$ and $K_e \in \Re^{3\times3}$ are the viscosity and the stiffness metrics of the environment, respectively, and $\dot{x}_s \in \Re^3$ and $x_s \in \Re^3$ are the velocity and position of the slave manipulator, respectively. A minus sign in the force means that the force's direction is against the operator.

An impedance-type control is implemented for the input to the slave as

$$\tau_s = C_{m,\text{pos}}\dot{x}_m - C_{s,\text{local}}\dot{x}_s - f_s \tag{5}$$

using (4), where $\dot{x}_m \in \Re^3$ is the velocity of the master. The force fed back to the operator is determined as follows:

$$f_m^{PP} = \frac{\left(Z_{cm}Z_{cs} + C_{m,\text{pos}}C_{s,\text{pos}}\right)\dot{x}_m - C_{s,\text{pos}}f_s}{Z_{cs}} \tag{6}$$

for the PP architecture and

$$f_m^{FP} = Z_{cm}\dot{x}_m + f_s \tag{7}$$

for the FP architecture, where $Z_{cm} = Z_m + C_{m,\text{local}}$ and $Z_{cs} = Z_s + C_{s,\text{local}}$. Finally, the control input to the master, τ_m, is calculated as

$$\tau_m^{PP} = -C_{m,\text{local}}\dot{x}_m + C_{s,\text{pos}}\dot{x}_s + f_m^{PP} \tag{8}$$

and

$$\tau_m^{FP} = -C_{m,\text{local}}\dot{x}_m - C_{s,\text{force}}f_s + f_m^{FP} \tag{9}$$

to produce the force defined in (6) and (7) for the PP and FP control architectures, respectively. The force feedback schemes are also explained in detail in ref. [13, 18].

2.4. Preliminary study using frequency domain analysis

As a preliminary study, a Bode plot analysis was performed for the functional analysis (in frequency domain) of the effects of the control methods and architectures on the teleoperator's perceptual ability. Bode plots of one of participants during the discrimination experiment with the reference environment, $Z_e = 10s + 1$, using the PP and FP control architectures are shown in Figs. 3(a) and (b), respectively.

It is noticeable that the perception-based method showed a more similar profile of magnitude than the other methods, so that the teleoperator can perceive environments more exactly using the perception-based method. As known from previous studies,[13, 14, 18, 23] the FP control architecture showed better impedance matching with the environment impedance than the PP control architecture for all control methods. The perception-based method, interestingly, transmitted higher and lower magnitude impedance with the PP and FP control architectures than the other methods, respectively. This means that higher force feedback does not guarantee better perception; therefore, just increasing control parameters (e.g., K_D, K_P, and K_f in this study) to increase the force feedback does not suffice to increase the teleoperator's perception.

Although the frequency domain analysis using the Bode plot is very helpful in seeing fundamental characteristics of the control methods and architectures, this analysis is not enough to evaluate the haptic teleoperation controllers well. The main reason is that the human's sensory-perceptual system cannot be characterized using several plots because human, generally, perceive environments via a series of information in a spatial and temporal domain. Moreover, it is very difficult to quantitatively evaluate a proposed control method and compare its performance with other methods using this analysis. Therefore, psychophysical experiments were conducted to evaluate the control methods and architectures from human perspective.

3. Methods

3.1. Participants

Ten healthy subjects (age range: 22–30 years; 9 males) with different backgrounds participated in the experiments. All subjects were right-handed by self-report and had normal or corrected to normal vision. Six of the subjects had a technical background but no knowledge of haptics and psychophysics,

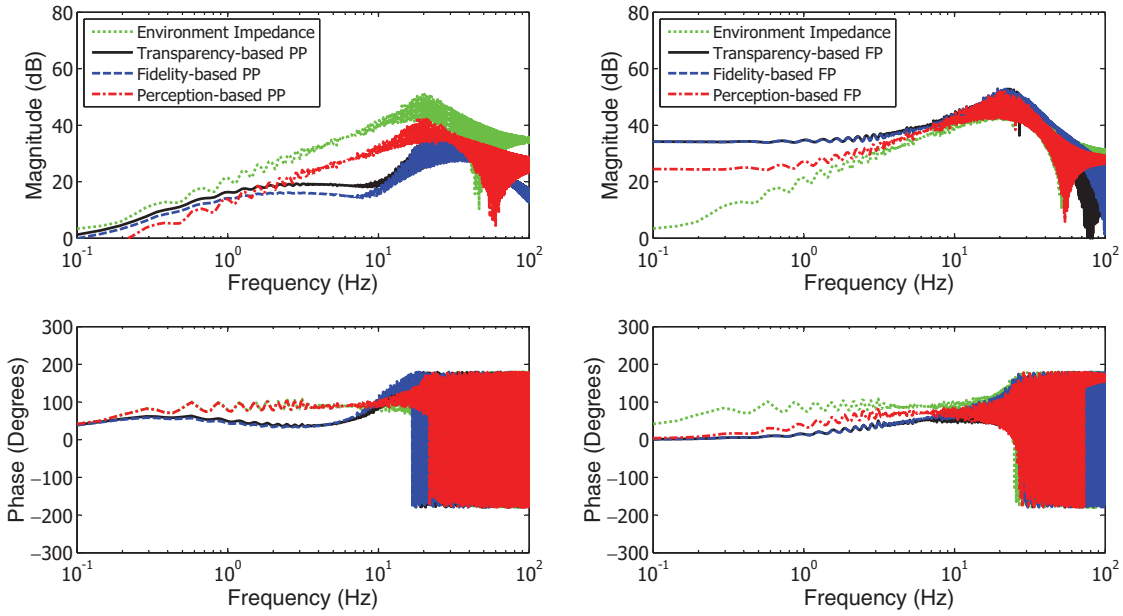

Fig. 3. (Colour online) Bode plot of environment impedance and transmitted impedances to operator using the transparency-based, fidelity-based, and perception-based methods. The force–position (FP) control architecture shows higher magnitude and better impedance matching with the environment impedance than the position–position (PP) control architecture. (a) Using the PP control architecture, the perception-based method transmits higher magnitude of impedance than the other methods. (b) Using the FP control architecture, the perception-based method transmits better matched impedance with the environment impedance than the other methods.

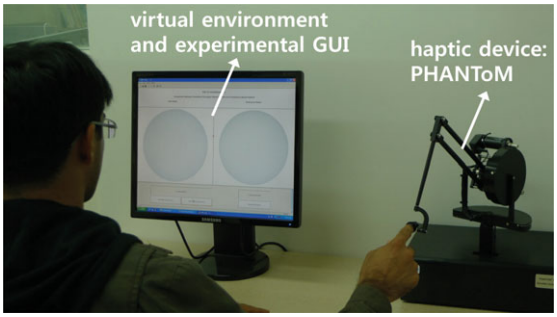

Fig. 4. (Colour online) Experimental setup for viscosity perception. The subject performs the experiment using the PHANToM haptic device with virtual environments using the index finger.

while the others were familiar with haptics. All participants gave informed consent prior to the study according to the 1964 Declaration of Helsinki.

3.2. Apparatus

Two kinds of experiments were conducted. One of them is the test of viscosity detection ability, while the other is the test of viscosity discrimination ability. The experimental setup is shown in Fig. 4. The human subject manipulates a PHANToM Premium 1.0 haptic device through a thimble-gimble interface using his or her index finger tip. The slave is implemented as a virtual manipulator which moves within a virtual environment. The teleoperation setup is implemented using Visual C++. Graphical user interfaces (GUIs) were made to test detection and discrimination ability while interacting with the virtual viscous environment as shown in Figs. 5(a) and (b). Without loss of general applicability, the experiments were implemented using virtual viscoelastic environments instead of real (physical) environments due to the large number of environments with varied viscosities needed

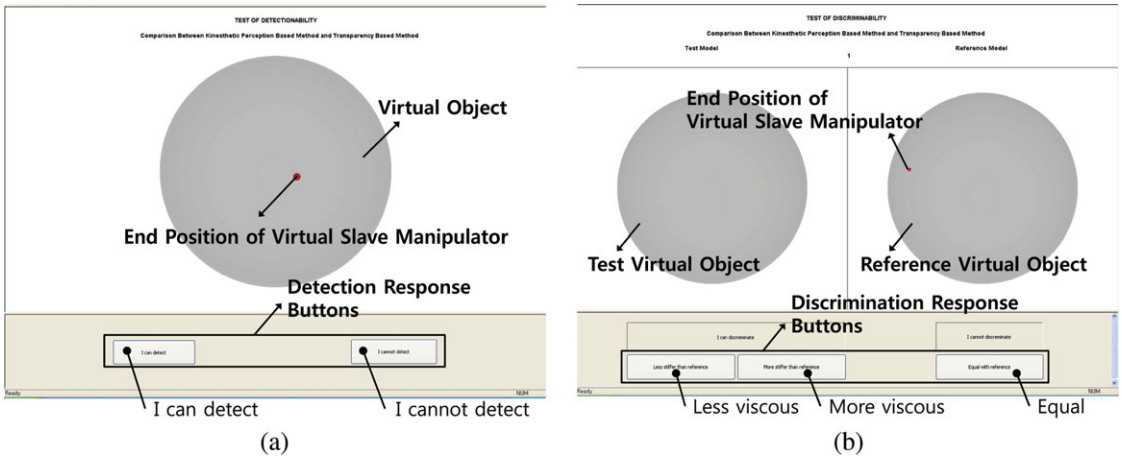

Fig. 5. (Colour online) Graphical user interfaces (GUIs) for the experiment. The subject responds whether he or she can detect and discriminate viscosity of virtual objects by pushing the appropriate response buttons. (a) GUI for the viscosity detection test. (b) GUI for the viscosity discrimination test.

to effectively perform the psychophysical experiments to find human operator's viscosity detection and discrimination thresholds.

The haptic update rate was fixed at 1 kHz for the PHANToM haptic device in order to achieve high-fidelity haptic feedback. Numerical differentiation of the position measured by the encoders of the haptic device was used to determine velocity. A second-order low-pass filter with a cut-off frequency of 40 Hz[21] was designed to filter the noise in the numerical differentiation. Similarly, the velocity of the slave is also calculated for (4).

One virtual environment was used for the detection test and the subjects were asked to indicate whether they could detect the viscosity of the environment or not, as shown in Fig. 5(a). For the discrimination test, however, there were two virtual environments, and the subjects were asked to discriminate between these two environments, relying on the haptic information that was fed back to them. The experiments used a within-subject design[27] (i.e., same subjects were participated all experiments) for cost efficiency and uniformity.

3.3. Haptic controller

In order to mutually compare methods, the experimental procedure requires the design of haptic teleoperation controllers for the transparency-based, the fidelity-based, and the perception-based methods. Initially, two local position controllers, $C_{m,\mathrm{local}}$ and $C_{s,\mathrm{local}}$, were designed based on the dynamics of the haptic device and the slave manipulator. Then the haptic controllers were designed on the basis of $C_{m,\mathrm{local}}$ and $C_{s,\mathrm{local}}$, by following the transparency-optimized control law and system stability.[12,13]

In this study, the master impedance is mathematically expressed as $Z_m = 0.072s^2$, which is similar to that of the PHANToM, while the slave manipulator is modeled as a PHANToM with a small surgical tool (300 g) whose impedance is given by $Z_s = 0.372s^2$.[28] The PD controller is implemented for all position controllers as explained in Section 2. Therefore, the design of the haptic controller is based on optimization of control parameters (i.e., K_D, K_P, and K_f) to maximize the performance (i.e., the transparency, the fidelity, and the perception). A steepest-descent algorithm[29] was used to optimize the controllers. The programming language C++ was chosen for a more effective computation of the optimization algorithm and was interfaced with MATLAB, using the function *fmincon* for optimization. A teleoperation simulator was made in VC++, which was also used to program a user-friendly interface to perform the simulations with varied conditions and model parameters.

For the transparency-based controllers, first, the initial values of the master and slave local position controllers were chosen according to Z_m, Z_s, and the values proposed in ref. [13]. Those values were then tuned by a grid search aimed at looking for all possible controller combinations offering good slave/master position tracking and system stability. Initializing the optimization with those

Table I. Summary of designed haptic controllers for the PP control architecture.

Control methods	$C_{m,\text{local}}$	$C_{s,\text{local}}$	$C_{m,\text{pos}}$	$C_{s,\text{pos}}$
Transparency-based	$2.5s + 50$	$15s + 330$	$2.5s + 50$	$-2.5s - 50$
Fidelity-based	$2.5s + 50$	$60.37s + 69.63$	$60.37s + 69.63$	$-2.5s - 50$
Perception-based	$5s + 60.04$	$10.37s + 138.04$	$10.37s + 138.04$	$-5s - 60.04$

Table II. Summary of designed haptic controllers for the FP control architecture.

Control methods	$C_{m,\text{local}}$	$C_{s,\text{local}}$	$C_{m,\text{pos}}$	$C_{s,\text{force}}$
Transparency-based	$2.5s + 50$	$15s + 330$	$5s + 330$	1
Fidelity-based	$2.5s + 50$	$131.58s + 98.41$	$31.58s + 98.41$	1
Perception-based	$2.21s + 15.59$	$13.74s + 336.01$	$113.74s + 336.01$	1

values, we obtained $C_{m,\text{local}} = 2.5s + 50$ and $C_{s,\text{local}} = 15s + 330$ (in the form of PD controller). The haptic controllers were then selected on the basis of the transparency-optimized law as explained in Section 2.2.1. The initial values of all the local position controllers for the fidelity-based and perception-based methods were identical with the transparency-based controllers. These controllers were optimized to maximize P_{fidelity} and $P_{\text{perception}}$ defined in (2) and (3) for the fidelity-based and perception-based methods, respectively, with the same low-pass filter for $W_{\text{perception}}$ used for the numerical differentiation. The haptic controllers were then chosen accordingly.

For both the fidelity and perception methods, the optimization problem applies the same stability conditions presented in ref. [18] and derived using Llewellyn's absolute stability criteria[30] for the mutual comparison. Finally, the designed haptic controllers based on the transparency-based, fidelity-based, and perception-based methods with both the PP and FP control architectures are summarized in Tables I and II.

3.4. Procedure

We designed a procedure to test human performance on the six possible controllers (three haptic teleoperation control methods using PP and FP architectures) with regard to viscosity detection (experiment 1) and discrimination (experiment 2) based on the most conventional psychophysical method, the method of limits.[26] Detection ability was tested by performing four *trials* (two cases $\times$ two series) for each controller, while discrimination ability was tested running 10 trials (five cases $\times$ two series) for each controller. The *cases* differed from each other in terms of the intensity of reference viscosity. The purpose of several cases was to encourage the participant to make perceptual judgments, as opposed to submitting intelligent guesses. Each case was further divided into ascending and descending *series*, as defined by the method of limits. The cases and series were fully randomized, which minimized response bias. Thus, each participant was required to perform 24 trials (six controllers $\times$ four trials) on the experiment 1 and 60 trials (six controllers $\times$ ten trials) on the experiment 2.

At the beginning of the experiment, the subjects were given a detailed tutorial and were provided with a small training session to become familiarized with PHANToM.

3.4.1. Experiment 1—Test of viscosity detection. Here, the human subjects were asked to interact with the virtual environment, which is referred to as the *test model*, and to respond if they could detect the viscosity of the environment or not.

For the ascending series of each case, the starting viscosity of the test model (lower limit) was set to 0 Ns/m and was hence undetectable for all subjects. After each trial the subject clicked the button to indicate whether he or she was able to detect the current impedance of the test model, and after the response the test model viscosity was increased by a fixed step size (0.05 or 0.10 Ns/m, respectively, case 1 and 2). The trial ended when the viscosity reached the upper limit, which was defined as either 1 (case 1) or 2 Ns/m (case 2). For the descending series, the initial viscosity (upper limit) was far beyond the detection threshold for humans, so the subjects felt the initial environment to be quite viscous. In this study, the upper limit was set to 1 Ns/m, the same as with the ascending series. The

viscosity of the test model was decreased by a fixed step size after each response, by either 0.05 or 0.10 Ns/m. The trial ended when the lower limit (0 Ns/m) was reached.

The points at which the response changed from *I Cannot Detect* to *I Can Detect* (for the ascending series) or from *I Can Detect* to *I Cannot Detect* (for the descending series) were marked as transition points.

3.4.2. Experiment 2—Test of viscosity discrimination. The test of discrimination ability made use of two virtual environments: the *test model* and the *reference model*. Each subject was asked to respond if he or she could discriminate between the viscosity of the test model and that of the reference model. Every subject had to perform the experiments for five different cases in which the reference models had five different environmental viscosities. The values of the reference model viscosity were chosen uniformly such that $B_e = 5$, 15, 25, 35, and 45 Ns/m.[18,24,31] As with the test of detection, there were two kinds of series for each of these reference models: the ascending series and the descending series. The upper limits, lower limits, and step sizes were set to 160%, 40%, and 5% of the reference viscosities for both series.

For the ascending series, the initial viscosity of the test model was much lower than that of the reference model. After the participant submitted his response, the test model viscosity increased while the reference model viscosity remained the same. This process went on until an upper limit was reached. At some point in this process, the human response was expected to switch from *less viscous* to *equal*. This point was marked as the lower limen (L_l). After more trials, the response was expected to switch from *equal* to *more viscous*, and this point was marked as the upper limen (L_u). The series was stopped when the upper limit was reached.

For the descending series, the initial viscosity of the test model was much higher than that of the reference model. As the participant submitted his response, the test model viscosity was decreased while the reference model viscosity was maintained. During the experimental procedure, the response was first expected to switch from *more viscous* to *equal* and, subsequently, from *equal* to *less viscous*. These response transition points were termed L_u and L_l, respectively. The series ended when the lower limit was reached.

4. Experimental Results

4.1. Manipulation behavior of subjects

The manipulation behaviors of subjects, represented by the position and velocity of the haptic device, and the transmitted force to the subjects, are summarized in Fig. 6. The manipulation behaviors are classified into push and pull behaviors based on the velocity of the haptic device, i.e., positive velocity represents the push behavior while negative velocity means the pull behavior. It shows that all subjects used similar manipulation positions and velocities and were fed back similar force in the experiments across the control methods but there is a significant difference in the manipulation velocities as well as the transmitted forces across the control architectures.

The differences between the maxima and minima of the manipulation velocity among the tested controllers did not affect the experimental results significantly, since the perceived viscosity also depended on the transmitted force, which was proportional to the manipulation velocity as shown in (4) but it would be strongly affected by the control methods and architectures as presented in Section 2.3 (see (6)–(9)). The manipulation behaviors will be analyzed and discussed in detail in Section 5.1.

4.2. Experiment 1—Test of viscosity detection

The experimental results are summarized in Fig. 7. There was a significant main effect of the controller method but not architecture ($F(2, 18) = 26.8$, $p < 0.001$). In addition, there is a statistically significant interaction ($F(2, 18) = 24.5$, $p < 0.001$). The detailed results are presented in the following subsections.

4.2.1. Control method. Our comparison results support the following conclusions (see Table III). Fidelity-based and perception-based controllers result in better detectability of viscosity than transparency-based controllers, but only among PP controllers. Overall, a transparency PP-based controller resulted poorest detection performance (mean: 1.0 ± 0.15 Ns/m). In contrast,

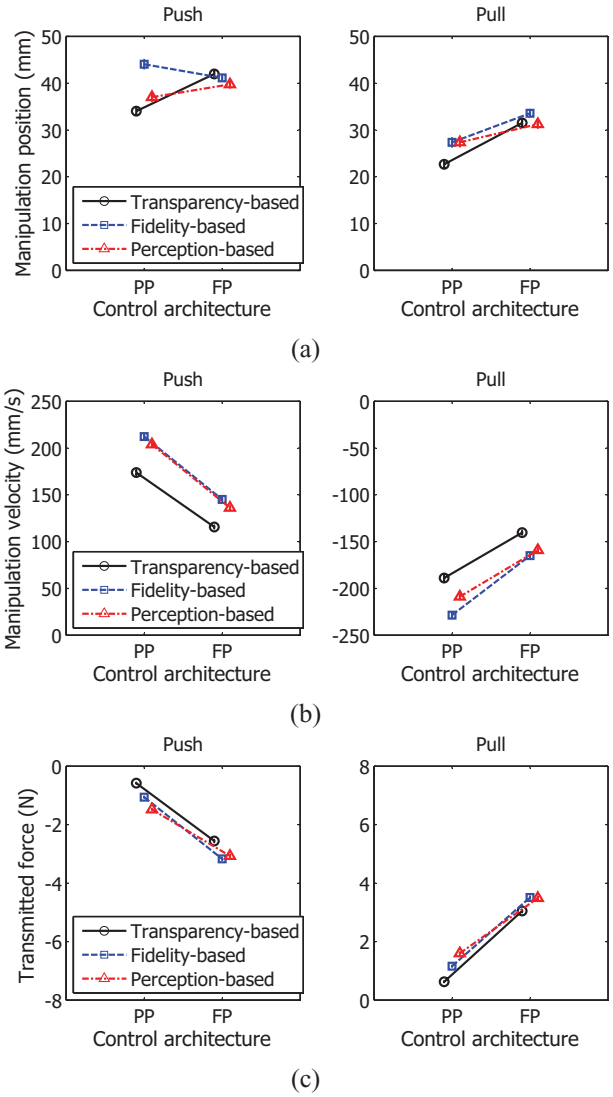

Fig. 6. (Colour online) Manipulation behavior of the human operator of all subjects, represented as mean ± standard deviation. Push and pull behaviors represent the manipulation of the haptic device with positive and negative velocity (i.e., maneuver the device forward and against to environments), respectively. (a) Manipulation positions, (b) manipulation velocities, and (c) transmitted forces.

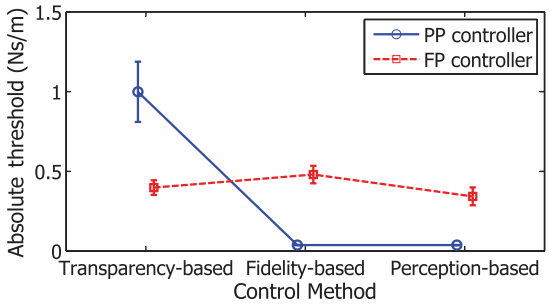

Fig. 7. (Colour online) Summary of experimental results for the viscosity detection test. Error bars indicated standard error of the population mean. The perception-based method shows the lowest absolute threshold in both the PP and FP control architectures. The transparency-based method has worst detection ability among the PP control architectures, while the fidelity-based method shows worst detection ability among the FP control architectures.

Table III. Quantitative evaluation of the detection ability test.

Control			Enhancement ratio R	Statistical analysis	
Common factor		Comparison		$t(1, 9)$	p-value
Control architecture	PP controller	Transparency-based vs. fidelity-based	−96.3%	5.07	< 0.001
		Transparency-based vs. perception-based	−96.3%	5.07	< 0.001
		Fidelity-based vs. perception-based	0.0%	–	–
	FP controller	Transparency-based vs. fidelity-based	20.8%	−3.43	< 0.01
		Transparency-based vs. perception-based	−13.8%	2.51	< 0.05
		Fidelity-based vs. perception-based	−28.7%	5.40	< 0.001
Control method	Transparency-based	PP vs. FP	−60.2%	3.68	< 0.01
	Fidelity-based	PP vs. FP	1180.0%	−8.20	< 0.001
	Perception-based	PP vs. FP	813.3%	−5.36	< 0.001

fidelity-based (mean: 0.04 ± 0.01 Ns/m) and perception-based (mean: 0.04 ± 0.01 Ns/m) PP controllers produced the best detection performance in our participants.

Among the PP controllers, the perception-based method produces a 96.3% enhancement in detection ability compared with the transparency-based method ($t(1, 9) = 5.07$, $p < 0.001$). With the FP controllers, the perception-based method produces a 13.8% enhancement ($t(1, 9) = 2.51$, $p < 0.05$) compared with the transparency-based method and a 28.7% enhancement ($t(1, 9) = 5.40$, $p < 0.001$) compared with the fidelity-based method.

4.2.2. Control architecture. In previous studies, the FP control architecture tended to result in better detection than PP for the property of stiffness, independent of the chosen control method.[18,23] Our findings on viscosity detection agree with this, to some extent. The transparency-based FP control architecture also shows a 60.2% enhancement in viscosity detection ability compared with the transparency-based PP controller ($t(1, 9) = 3.68$, $p < 0.01$). However, it is also worth noting that viscosity detection was actually better for the fidelity-based ($t(1, 9) = 8.20$, $p < 0.001$) and perception-based methods ($t(1, 9) = 5.36$, $p < 0.001$) in the PP control architecture.

4.2.3. Discussion. Experimental results show that the perception-based control method is the most consistent in yielding good viscosity detection, regardless of the control architecture. The fidelity-based method does not guarantee an enhancement of viscosity detection. In fact, detection was significantly inferior for fidelity-based methods with FP controllers, relative to the perception-based method. Also, the enhancement of detection performance is lower when using the fidelity-based method than using the perception-based method, relative to the transparency-based method.

The transparency-based method exploits two well-known facts. First, force information from the slave side is helpful in improving force tracking.[13] Second, slave force information increases stiffness detection ability as well as force tracking.[18,23] While our findings show that force information does result in better viscosity detection with a transparency-based method, a significantly better performance can be achieved by providing position information, using fidelity-based and perception-based methods instead.

It is important to note that this reported enhancement is sensitive to the initial values that were chosen for the optimization of the controller.

4.3. Experiment 2—Test of viscosity discrimination

The same participants performed a follow-up experiment on viscosity discrimination. Discrimination performance was measured in terms of JND, for which lower values indicated better discrimination. The mean JNDs are summarized by Fig. 8 for the different controllers, across the different levels of reference stimuli viscosity.

From this, it is worth noting that the perception-based FP controller resulted in the lowest JND, while the transparency-based PP controller resulted in the highest JND. Our computed measures of JND ranged from 9% to about 30%, which were comparable to those obtained in previous studies on viscosity perception.[6,32]

Table IV. Quantitative evaluation of discrimination ability test.

Control				Statistical analysis	
Common factor		Comparison	Enhancement ratio R	$t(1,9)$	p-value
Control architecture	PP controller	Transparency-based vs. fidelity-based	−8.1%	0.89	> 0.05
		Transparency-based vs. perception-based	−34.0%	4.02	< 0.01
		Fidelity-based vs. perception-based	−28.1%	3.75	< 0.01
	FP controller	Transparency-based vs. fidelity-based	−17.5%	3.85	< 0.01
		Transparency-based vs. perception-based	−37.5%	5.44	< 0.001
		Fidelity-based vs. perception-based	−24.3%	3.36	< 0.01
Control method	Transparency-based	PP vs. FP	−16.3%	1.68	> 0.05
	Fidelity-based	PP vs. FP	−24.8%	3.23	< 0.05
	Perception-based	PP vs. FP	−20.8%	3.40	< 0.01

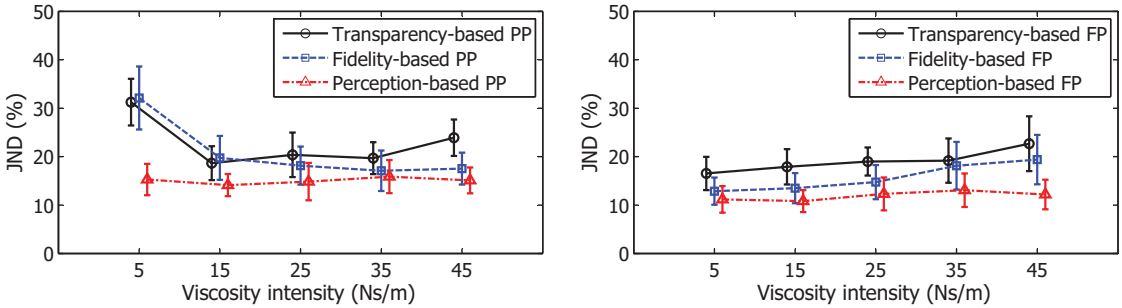

Fig. 8. (Colour online) Experimental results for the viscosity discrimination test in just noticeable difference (JND) with various reference viscosity intensities, represented as mean ± standard error. The perception-based method showed the lowest JND for all reference viscosity intensities in both the PP and FP control architectures. (a) PP control architecture and (b) FP control architecture.

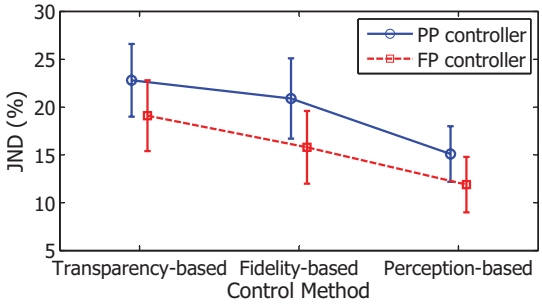

Fig. 9. (Colour online) Summary of experimental results for the viscosity discrimination test. Error bars indicated standard error of the population mean. The perception-based method showed a lower JND than the transparency-based and fidelity-based methods in both PP and FP control architectures.

The results of our repeated measures ANOVA are summarized in Fig. 9 and Table IV. Our analysis revealed statistically significant main effects for both factors of the control architecture ($F(1,9) = 11.1$, $p < 0.01$) and control method ($F(1,9) = 20.1$, $p < 0.001$). Also, there was no significant interaction between these two factors. Therefore, the pattern of results across the control methods can be inferred to be similar for both control architectures.

4.3.1. Control method. Perception-based controllers consistently yielded the best discrimination performance. In the case of the PP control architecture, the perception-based method shows a discrimination ability enhancement of 34.0% compared with the transparency-based method ($t(1,9) = 4.02$, $p < 0.01$), and of 28.1% in comparison to the fidelity-based method ($t(1,9) = 3.75$, $p < 0.01$). The same pattern of response is noted for the FP control architecture, the

perception-based method shows a discrimination ability enhancement of 37.5% in comparison to the transparency-based method ($t(1, 9) = 5.44$, $p < 0.001$), and of 24.3% compared with the fidelity-based method ($t(1, 9) = 3.36$, $p < 0.01$).

Fidelity-based controllers yielded better discrimination than transparency-based controllers, but this was statistically significant only with the FP control architecture. Fidelity-based controllers in the PP control architecture showed a 8.1% enhancement of JND in comparison to the transparency-based method ($t(1, 9) = 0.89$, $p > 0.05$). For FP control, the fidelity-based method also shows a 17.5% enhancement of JND compared with the transparency-based method ($t(1, 9) = 3.85$, $p < 0.01$).

4.3.2. Control architecture. The FP control architecture consistently yields better discrimination in our participants' performance compared with the PP architecture. This finding is consistent with the stiffness discrimination tests presented in refs. [18, 23]. More specifically, our planned comparisons of FP control with PP control indicated that JND decreases by 20.8% ($t(1, 9) = 3.40$, $p < 0.01$) for the perception-based method. However, JND decreases of the FP controller compared with the PP controller are not significant for the transparency-based and fidelity-based methods, respectively. It is interesting to note that even though the PP control architecture is optimized for the perception-based method, a perception-based method appears to induce better discrimination performance for the FP control architecture, which is tuned for the transparency-based and fidelity-based methods.

4.3.3. Discussion. Generally speaking, the following inferences can be made. FP controllers facilitated better discrimination performance in our participants than PP controllers. In addition, discrimination performance is best for controllers that were optimized for perception, relative to those that were designed for fidelity and transparency instead. In turn, fidelity-based controllers resulted in better discrimination performance than transparency-based controllers.

The results of the viscosity discrimination test in Experiment 2 agree with those reported by Son *et al.*[18,23] on stiffness discrimination. Taken together, slave force information increases discrimination performance for both stiffness and viscosity perception. This is especially so with the perception-based method.

5. General Discussions

5.1. Manipulation behavior

There is no significant difference in manipulation positions (x_m) across the control methods and architectures, as shown in Fig. 6(a), which meant that the subject's workspace during the experiments was similar. In the manipulation velocities ($\dot{x}_m$) shown in Fig. 6(b), however, there was a significant difference across the control architectures while significantly no difference across the control methods. It is worth noting that, in general, humans move their hand faster when perceiving a less viscous environment, as reported in ref. [6]. This natural behavior in humans was also observed in this study. The subjects manipulated the haptic device faster with the PP control architecture than with the FP one for all control methods. It is obvious that the main reason for this is that they have more difficulties in perceiving test environments with the PP control architecture than the FP one, as found and analyzed in Section 4. This manipulation behavior of subjects is consistent with the previous study.

It is very important to note that the transmitted forces (f_m) using the PP control architecture were not higher (actually, significantly lower) than the forces using the FP control architecture, as shown in Fig. 6(c). However, $\dot{x}_m$, using the PP control architecture, were higher than the FP one; and the interacting force (f_s) to be transmitted to the subject is proportional to the velocity of the slave ($\dot{x}_s$), which is a function of $\dot{x}_m$ (see (4) and (5)). The main reason for this is that $\dot{x}_s$ is also affected by the haptic and local controllers (i.e., $C_{m,\text{pos}}$ and $C_{s,\text{local}}$) as well as f_s. Additionally, f_m is determined not only by f_s and $\dot{x}_m$ but also by several haptic and local controllers, as shown in (6) and (7). We can, therefore, conclude that the control architecture **gave more contributions on the transmitted force than the manipulation velocities.

5.2. Effects of the control method

The transparency-based method was proposed to match the transmitted impedance (especially, viscosity in this study) to the operator (Z_{to}) to be close with the environment impedance (Z_e). However, practically, it is impossible to achieve perfect transparency due to the nonlinearity of the

system, disturbances, modeling errors, and a possible time delay between the master and the slave. Even if, theoretically, we achieve perfect transparency using the transparency-based method, it is very difficult to detect and discriminate environments precisely for a case in which two surrounding tissues differ by distinguishable impedances as far as the magnitude is concerned while they individually have very small impedances difficult to be detected (e.g., impedances falling out to human's AL).

From this perspective, the fidelity-based method was proposed, which is a pioneer research regarding the enhancement of the fidelity measure for a teleoperation system interacting with soft tissues. However, while the fidelity-based method focuses on enhancing the fidelity, the focus of the perception-based method is toward enhancing teleoperator's perception capabilities, which is very essential for an effective and successful teleoperation (especially, telesurgical) procedure. Therefore, the enhancement of detection and discrimination abilities, using the fidelity-based method, is much less than our perception-based method, as is evident from the experimental results. This is probably because the fidelity-based method tried to increase only the fidelity, which measures the sensitivity of the transmitted impedance to changes in the environmental impedance ($\frac{\Delta Z_{to}}{\Delta Z_e}$, see (2)), and is different from the concept of the JND. Unfortunately, this approach ignores a fundamental concept in perceptual psychophysics. According to Weber's law,[26] the JND varies with the initial intensity of impedance, a finding also shown in the current results and, therefore, it might be more appropriate to use the perception measure, $P_{\text{perception}}$, which measures the sensitivity of the relative change of the transmitted impedance to relative changes in the environment impedance ($\frac{\Delta Z_{to}/Z_{to}}{\Delta Z_e/Z_e}$, see (3)) for enhancing the discrimination ability or the JND.

In addition, the perception-based method helps to increase the detection ability (via M_{det} in (3)) for an environment with very small impedance like that of microsurgical applications, as is evident from the results. In Fig. 6(c), we can also see that, generally, the fidelity-based and perception-based methods transmitted higher force than the transparency-based method, which can offer better detection. However, it is difficult to analyze discrimination ability using Fig. 6 presented in time domain, and we present a frequency domain analysis in Section 2.4.

5.3. Effects of force information from the slave manipulator

It is well known that force information from the slave side is helpful in improving force tracking;[13] slave force information increases impedance perception ability as well as force tracking.[23] Our experimental results in Section 4 also exploited this fact. Manipulation behaviors shown in Fig. 6 are also worth seeing the contribution of the slave force information on higher force feedback, as discussed in the previous subsection.

However, force sensors, which can measure the interaction force feeding back to the surgeon, are difficult to use in surgical cases, mainly because they are mostly positioned outside the body due to their large size, which can result in picking up unwanted friction forces and eventual distortion of force information.[25,33,34] A force sensor, if somehow placed inside, can also lead to potential issues due to blood clotting and eventual insulation problems. Note that, recently, a compact and precise force/torque sensors have actively been developed for telesurgical applications;[35–38] however, these are still not common in applications that generally use an industrial manipulator as the slave.

Note also that the PP control architecture shows more robustness in system stability than the FP control architecture, while it shows worse performance.[13] Therefore, the selection of a proper control architecture among the PP and FP ones has to be made according to its applications by considering the performance–stability tradeoff.

5.4. Limitations of control methods

In this study, the master and the slave were modeled using only inertia terms to optimize the control methods. In practical cases, however, a general nonlinear dynamic model, including velocity-dependent terms and position-dependent terms, needs to be considered to increase teleoperator's perception performance. One possible solution to this problem can be achieved by using appropriate disturbance observers which can cancel the unmodeled terms and can give expected behavior with the inertia terms only.

In addition, the fidelity-based and perception-based methods might not work adaptively with sudden and significant changes in the environment impedance. Therefore, an adaptive control scheme has to be added to the control methods, which would enhance both the detection and discrimination

abilities for an environment with small impedance while enhancing only the discrimination ability for hard and rigid environments. However, the focus of this paper is toward tele-microsurgical or telesurgical cases dealing with soft tissue environments, where surgeons operate with carefully controlled motions, and, in those cases, sudden significant changes in the environment impedance might not occur.

It is also worth studying the detection and discrimination experiments presented here by using real soft tissues and a slave manipulator (as in our previous study for stiffness perception[18]) to see and analyze other possible factors on the performance of the perception-centered methods. This is left for further study.

6. Conclusion

Viscosity detection and discrimination tests were performed to characterize the effect of control methods and haptic information on viscosity perception in haptic teleoperation systems. Our experiments using haptic teleoperation systems with the thimble-gimbal interface can be summarized as follows:

- The perception-based teleoperation control method consistently enhanced both the detection and discrimination performance of human operators, relative to the transparency-based and fidelity-based methods, by decreasing the AL and the JND measures.
- The fidelity-based teleoperation control method generally enhanced detection and discrimination performance, relative to the transparency method. However, this enhancement was not consistent.
- The slave manipulator's force information contributed significantly to decrease the AL in the viscosity detection test for all methods (transparency-based, fidelity-based, and perception-based).
- Force information from the slave manipulator helps to significantly increase the discrimination ability of human operators when using the perception-based method, but is not helpful in the case of the transparency-based and fidelity-based methods.

These current observations demonstrate how a psychophysical approach can enhance haptic teleoperation system control for viscosity perception. In addition, the use of force information from the slave manipulator increases viscosity discrimination ability, as would have been expected from theoretical considerations.

Acknowledgments

The authors thank Dr. Antonio Franchi and Dr. Lewis Chuang, Max Planck Institute for Biological Cybernetics, for constructive comments.

This research was supported by a Korea Research Foundation grant funded by the Korean government (NRF-2011-357-D00003), the Brain Korea 21 Project in 2008-2011, the Max Planck Society, and the WCU (World Class University) program funded by the Ministry of Education, Science and Technology, through the National Research Foundation of Korea (R31-10008).

References

1. O. van der Meijden and M. Schijven, "The value of haptic feedback in conventional and robot-assisted minimal invasive surgery and virtual reality training: A current review," *Surg. Endosc.* **23**(6), 1180–1190 (2009).
2. J. Hill, P. Holst, J. Jensen, J. Goldman, Y. Gorfu and D. Ploeger, "Telepresence interface with applications to microsurgery and surgical simulation," *Stud. Health Technol. Inform.* **50**, 96–102 (1998).
3. F. Tendick, S. Sastry, R. Fearing and M. Cohn, "Applications of micromechatronics in minimally invasive surgery," *IEEE/ASME Trans. Mechatronics* **3**(1), 34–42 (1998).
4. E. Heijnsdijk, A. Pasdeloup, A. Van der Pijl, J. Dankelman and D. Gouma, "The influence of force feedback and visual feedback in grasping tissue laparoscopicauy," *Surg. Endosc.* **18**(6), 980–985 (2004).
5. L. A. Jones, "Kinesthetic Sensing," **In**: *Human and Machine Haptics* (M. Cutkosky, R. Howe, K. Salisbury and M. Srinivasan, eds.) (MIT Press, Cambridge, MA, 2000).
6. L. Jones and I. Hunter, "A perceptual analysis of viscosity," *Exp. Brain Res.* **94**(2), 343–351 (1993).
7. F. Huang, J. Patton and F. Mussa-Ivaldi, "Manual skill generalization enhanced by negative viscosity," *J. Neurophysiol.* **104**(4), 2008–2019 (2010).
8. C. Steele, P. Van Lieshout and D. Goff, "The rheology of liquids: A comparison of clinicians subjective impressions and objective measurement," *Dysphagia.* **18**(3), 182–195 (2003).

9. S. Lederman, R. Klatzky, C. Tong and C. Hamilton, "The perceived roughness of resistive virtual textures: II. Effects of varying viscosity with a force-feedback device," *ACM Trans. Appl. Perception* **3**(1), 15–30 (2006).
10. T. Sheridan, "Telerobotics," *Automatica* **25**(4), 487–507 (1989).
11. P. Hokayem and M. Spong, "Bilateral teleoperation: An historical survey," *Automatica* **42**(12), 2035–2057 (2006).
12. D. Lawrence, "Stability and transparency in bilateral teleoperation," *IEEE Trans. Robot. Autom.* **9**(5), 624–637 (1993).
13. K. Hashtrudi-Zaad and S. Salcudean, "Analysis of control architectures for teleoperation systems with impedance/admittance master and slave manipulators," *Int. J. Robot. Res.* **20**(6), 419–445 (2001).
14. M. Çavusoglu, A. Sherman and F. Tendick, "Design of bilateral teleoperation controllers for haptic exploration and telemanipulation of soft environments," *IEEE Trans. Robot. Autom.* **18**(4), 641–647 (2002).
15. G. De Gersem, H. Van Brussel and F. Tendick, "Reliable and enhanced stiffness perception in soft-tissue telemanipulation," *Int. J. Robot. Res.* **24**(10), 805–822 (2005).
16. P. Malysz and S. Sirouspour, "Nonlinear and filtered force/position mappings in bilateral teleoperation with application to enhanced stiffness discrimination," *IEEE Trans. Robot.* **25**(5), 1134–1149 (2009).
17. D. Botturi, M. Vicentini, M. Righele and C. Secchi, "Perception-centric force scaling in bilateral teleoperation," *Mechatronics* **20**(7), 802–811 (2010).
18. H. I. Son, T. Bhattacharjee and H. Hashimoto, "Enhancement in operator's perception of soft tissues and its experimental validation for scaled teleoperation systems," *IEEE/ASME Trans. Mechatronics* **16**(6), 1096–1109 (2011).
19. H. I. Son, T. Bhattacharjee and H. Hashimoto, "Effect of impedance-shaping on perception of soft tissues in macro-micro teleoperation," *IEEE Trans. Ind. Electron.* **59**(8), 3273–3285 (2012).
20. Y. Sun and B. Nelson, "Biological cell injection using an autonomous microrobotic system," *Int. J. Robot. Res.* **21**(10–11), 861–868 (2002).
21. N. Dhruv and F. Tendick, "Frequency Dependence of Compliance Contrast Detection," **In**: *Proceedings of the Symposium on Haptic Interfaces for Virtual Environment and Teleoperator Systems* (Orlando, FL, 2000) pp. 1087–1093.
22. A. Sherman, M. Çavusoglu and F. Tendick, "Comparison of Teleoperator Control Architectures for Palpation Task," **In**: *Proceedings of the Symposium on Haptic Interfaces for Virtual Environments and Teleoperator Systems* (Orlando, FL, 2000) pp. 1261–1268.
23. H. I. Son, T. Bhattacharjee, H. Jung and D. Y. Lee, "Psychophysical Evaluation of Control Scheme Designed for Optimal Kinesthetic Perception in Scaled Teleoperation," **In**: *Proceedings of the IEEE International Conference on Robotics and Automation* (Anchorage, AK, 2010) pp. 5346–5351.
24. H. I. Son, A. Franchi, L. Chuang, J. Kim, H. Bülthoff and P. Robuffo Giordano, "Human-Centered Design and Evaluation of Haptic Cueing for Teleoperation of Multiple Mobile Robots," *IEEE Trans. Syst. Man Cybern.* **43**(2), 597–609 (2013).
25. H. I. Son, T. Bhattacharjee and D. Y. Lee, "Estimation of environmental force for the haptic interface of robotic surgery," *Int. J. Med. Robot. Comput. Assist. Surg.* **6**(2), 221–230 (2010).
26. G. Gescheider, *Psychophysics: The Fundamentals* (Lawrence Erlbaum, Mahwah, NJ, 1997).
27. G. Keppel and T. Wickens, *Design and Analysis* (Prentice Hall, Englewood Cliffs, NJ, 2007).
28. N. Diolaiti, G. Niemeyer, F. Barbagli and J. Salisbury, "Stability of haptic rendering: Discretization, quantization, time delay, and coulomb effects," *IEEE Trans. Robot.* **22**(2), 256–268 (2006).
29. A. Belegundu and T. Chandrupatla, *Optimization Concepts and Applications in Engineering* (Prentice Hall, Upper Saddle River, NJ, 1999).
30. S. Haykin, *Active Network Theory* (Addison-Wesley, Reading, MA, 1970).
31. H. Woo, W. Kim, W. Ahn, D. Lee, and S. Yi, "Haptic interface of the KAIST-Ewha colonoscopy simulator II," *IEEE Trans. Inf. Technol. Biomed.* **12**(6), 746–753 (2008).
32. G. Beauregard, M. Srinivasan and N. Durlach, "The Manual Resolution of Viscosity and Mass," **In**: *Proceedings of the ASME Dynamic Systems and Control Division*, vol. **DSC-57-2**, (Ann Arbor, MI, 1995) pp. 657–662 .
33. M. MacFarlane, J. Rosen, B. Hannaford, C. Pellegrini and M. Sinanan, "Force-feedback grasper helps restore sense of touch in minimally invasive surgery," *J. Gastrointestinal Surg.* **3**(3), 278–285 (1999).
34. M. Tavakoli, A. Aziminejad, R. Patel and M. Moallem, "Methods and mechanisms for contact feedback in a robot-assisted minimally invasive environment," *Surg. Endosc.* **20**(10), 1570–1579 (2006).
35. J. Peirs, J. Clijnen, D. Reynaerts, H. Brussel, P. Herijgers, B. Corteville and S. Boone, "A micro optical force sensor for force feedback during minimally invasive robotic surgery," *Sensors Actuators A: Phys.* **115**(2–3), 447–455 (2004).
36. U. Seibold, B. Kubler and G. Hirzinger, "Prototype of Instrument for Minimally Invasive Surgery with 6-axis Force Sensing Capability," **In**: *Proceedings of the IEEE International Conference on Robotics and Automation* (Barcelona, Spain, 2005) pp. 496–501.
37. U. Seibold, B. Kubler, S. Thielmann and G. Hirzinger, "Endoscopic 3 Dof-Instrument with 7 Dof Force/Torque Feedback," **In**: *Workshop at the IEEE International Conference on Robotics and Automation* (Kobe, Japan, 2009) pp. 1–4.
38. U. Hagn, R. Konietschke, A. Tobergte, M. Nickl, S. Jörg, B. Kübler, G. Passig, M. Gröger, F. Fröhlich, U. Seibold, *et al.* "DLR mirosurge: A versatile system for research in endoscopic telesurgery," *Int. J. Comput. Assist. Radiol. Surg.* **5**(2), 183–193 (2010).